“Photonic crystals”

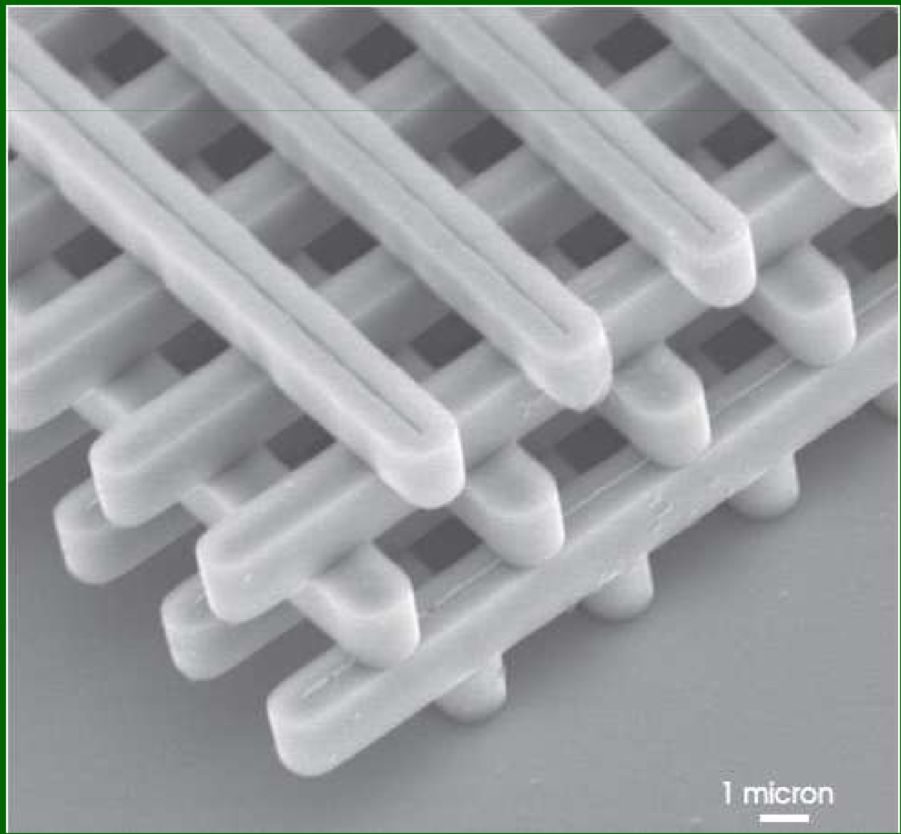

Composition and dimensionality of photonic crystals

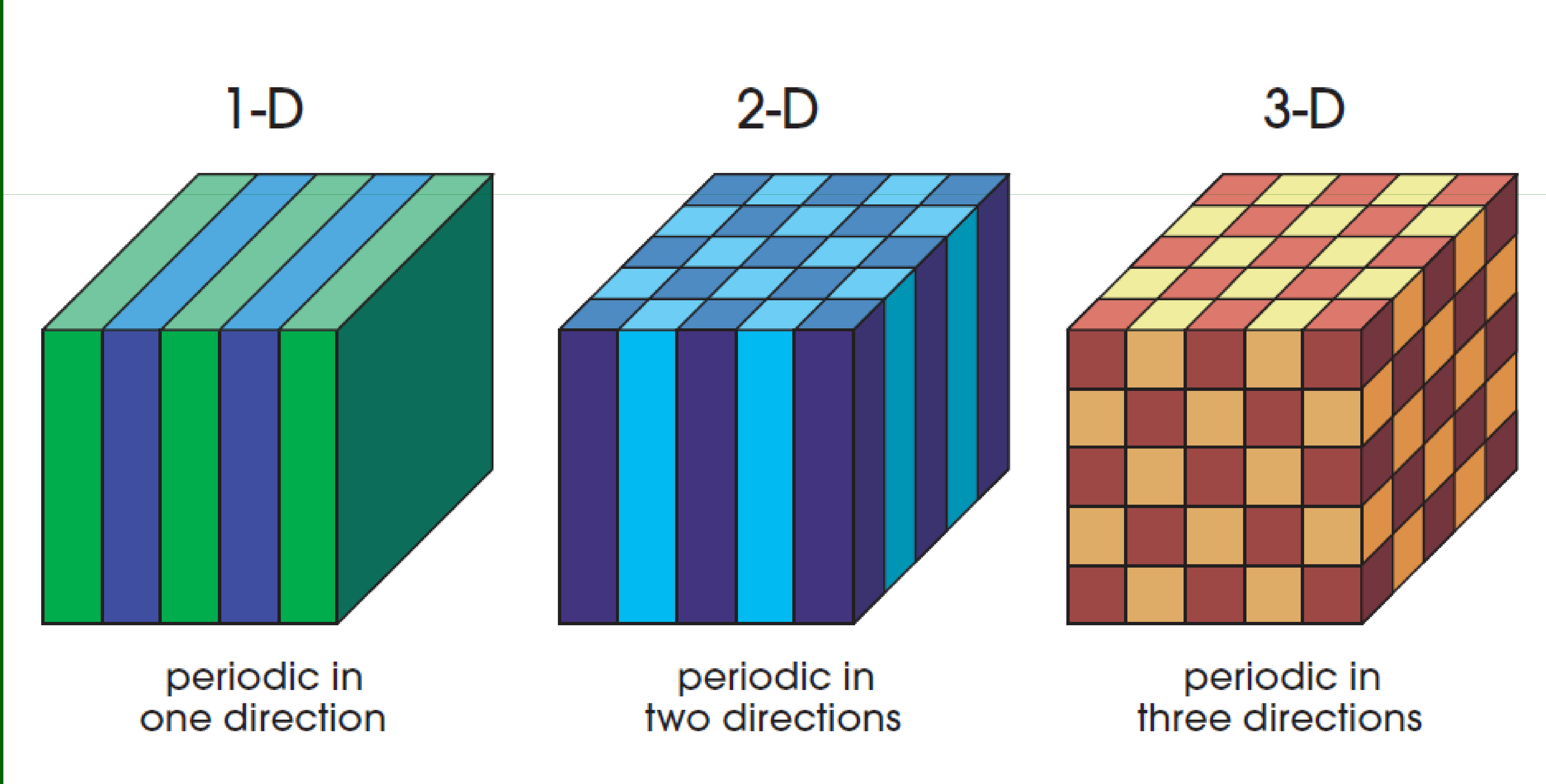

$$\nabla \cdot \mathbf{B} = 0 \quad \nabla \times \mathbf{E} + \frac{\partial \mathbf{B}}{\partial t} = 0$$

$$\nabla \cdot \mathbf{D} = \rho \quad \nabla \times \mathbf{H} - \frac{\partial \mathbf{D}}{\partial t} = \mathbf{J}$$

$$\mathbf{D}(\mathbf{r}) = \varepsilon_0 \varepsilon(\mathbf{r}) \mathbf{E}(\mathbf{r})$$

$$\mathbf{B}(\mathbf{r}) = \mu_0 \mu(\mathbf{r}) \mathbf{H}(\mathbf{r})$$

$$\mathbf{B} = \mu_0 \mathbf{H}$$

$$\nabla \cdot \mathbf{H}(\mathbf{r}, t) = 0 \qquad \nabla \times \mathbf{E}(\mathbf{r}, t) + \mu_0 \frac{\partial \mathbf{H}(\mathbf{r}, t)}{\partial t} = 0$$

$$\nabla \cdot [\varepsilon(\mathbf{r}) \mathbf{E}(\mathbf{r}, t)] = 0 \quad \nabla \times \mathbf{H}(\mathbf{r}, t) - \varepsilon_0 \varepsilon(\mathbf{r}) \frac{\partial \mathbf{E}(\mathbf{r}, t)}{\partial t} = 0.$$

$$\mathbf{H}(\mathbf{r},t) = \mathbf{H}(\mathbf{r})e^{-i\omega t}$$

$$\mathbf{E}(\mathbf{r},t) = \mathbf{E}(\mathbf{r})e^{-i\omega t}.$$

$$\nabla \cdot \mathbf{H}(\mathbf{r}) = 0, \quad \nabla \cdot [\varepsilon(\mathbf{r})\mathbf{E}(\mathbf{r})] = 0,$$

$$\nabla \times \mathbf{E}(\mathbf{r}) - i\omega\mu_0\mathbf{H}(\mathbf{r}) = 0$$

$$\nabla \times \mathbf{H}(\mathbf{r}) + i\omega\varepsilon_0\varepsilon(\mathbf{r})\mathbf{E}(\mathbf{r}) = 0.$$

$$\boxed{\nabla \times \left(\frac{1}{\varepsilon(\mathbf{r})}\nabla \times \mathbf{H}(\mathbf{r})\right) = \left(\frac{\omega}{c}\right)^2 \mathbf{H}(\mathbf{r}).}$$

$$\mathbf{E}(\mathbf{r}) = \frac{i}{\omega\varepsilon_0\varepsilon(\mathbf{r})}\nabla \times \mathbf{H}(\mathbf{r}).$$

$$\hat{\Theta}\mathbf{H}(\mathbf{r}) = \left(\frac{\omega}{c}\right)^2 \mathbf{H}(\mathbf{r}).$$

$$\hat{\Theta}\mathbf{H}(\mathbf{r}) \triangleq \nabla \times \left(\frac{1}{\varepsilon(\mathbf{r})}\nabla \times \mathbf{H}(\mathbf{r})\right)$$

	Quantum Mechanics	*Electrodynamics*
Field	$\Psi(\mathbf{r},t) = \Psi(\mathbf{r})e^{-iEt/\hbar}$	$\mathbf{H}(\mathbf{r},t) = \mathbf{H}(\mathbf{r})e^{-i\omega t}$
Eigenvalue problem	$\hat{H}\Psi = E\Psi$	$\hat{\Theta}\mathbf{H} = \left(\frac{\omega}{c}\right)^2 \mathbf{H}$
Hermitian operator	$\hat{H} = -\frac{\hbar^2}{2m}\nabla^2 + V(\mathbf{r})$	$\hat{\Theta} = \nabla \times \frac{1}{\varepsilon(\mathbf{r})}\nabla \times$

$$[\hat{O}_I, \hat{\Theta}]\mathbf{H} = \hat{O}_I(\hat{\Theta}\mathbf{H}) - \hat{\Theta}(\hat{O}_I\mathbf{H}) = 0$$

$$\Longrightarrow \hat{\Theta}(\hat{O}_I\mathbf{H}) = \hat{O}_I(\hat{\Theta}\mathbf{H}) = \frac{\omega^2}{c^2}(\hat{O}_I\mathbf{H}).$$

$$\hat{T}_{dz}e^{ikz} = e^{ik(z-d)} = \left(e^{-ikd}\right)e^{ikz}.$$

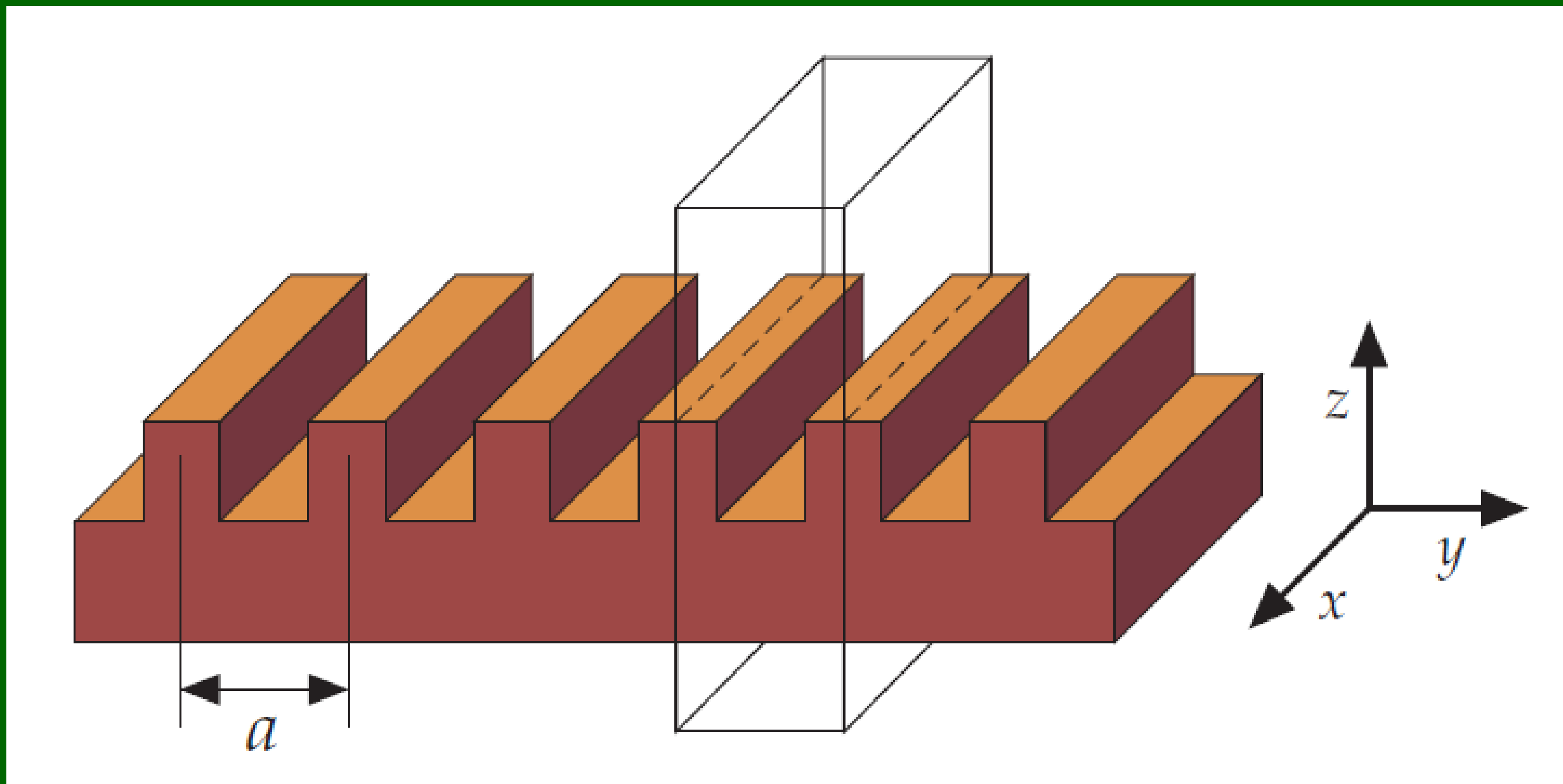

$$\hat{T}_{d\hat{\mathbf{x}}} e^{ik_x x} = e^{ik_x(x-d)} = \left(e^{-ik_x d}\right) e^{ik_x x}$$

$$\hat{T}_{\mathbf{R}} e^{ik_y y} = e^{ik_y(y-\ell a)} = \left(e^{-ik_y \ell a}\right) e^{ik_y y}.$$

$$\begin{aligned}\mathbf{H}_{k_x,k_y}(\mathbf{r}) &= e^{ik_x x} \sum_m \mathbf{c}_{k_y,m}(z) e^{i(k_y+mb)y} \\ &= e^{ik_x x} \cdot e^{ik_y y} \cdot \sum_m \mathbf{c}_{k_y,m}(z) e^{imby} \\ &= e^{ik_x x} \cdot e^{ik_y y} \cdot \mathbf{u}_{k_y}(y,z),\end{aligned}$$

$$\mathbf{H}(\ldots, y, \ldots) \propto e^{ik_y y} \cdot \mathbf{u}_{k_y}(y, \ldots).$$

$$\mathbf{k} = k_1\mathbf{b}_1 + k_2\mathbf{b}_2 + k_3\mathbf{b}_3$$

$$\mathbf{H}_{\mathbf{k}}(\mathbf{r}) = e^{i\mathbf{k}\cdot\mathbf{r}}\mathbf{u}_{\mathbf{k}}(\mathbf{r}),$$

$$\mathbf{u}_{\mathbf{k}}(\mathbf{r}) = \mathbf{u}_{\mathbf{k}}(\mathbf{r}+\mathbf{R})$$

	Quantum Mechanics	*Electrodynamics*
Discrete translational symmetry	$V(\mathbf{r}) = V(\mathbf{r}+\mathbf{R})$	$\varepsilon(\mathbf{r}) = \varepsilon(\mathbf{r}+\mathbf{R})$
Commutation relationships	$[\hat{H}, \hat{T}_{\mathbf{R}}] = 0$	$[\hat{\Theta}, \hat{T}_{\mathbf{R}}] = 0$
Bloch's theorem	$\Psi_{\mathbf{k}n}(\mathbf{r}) = u_{\mathbf{k}n}(\mathbf{r})e^{i\mathbf{k}\cdot\mathbf{r}}$	$\mathbf{H}_{\mathbf{k}n}(\mathbf{r}) = \mathbf{u}_{\mathbf{k}n}(\mathbf{r})e^{i\mathbf{k}\cdot\mathbf{r}}$

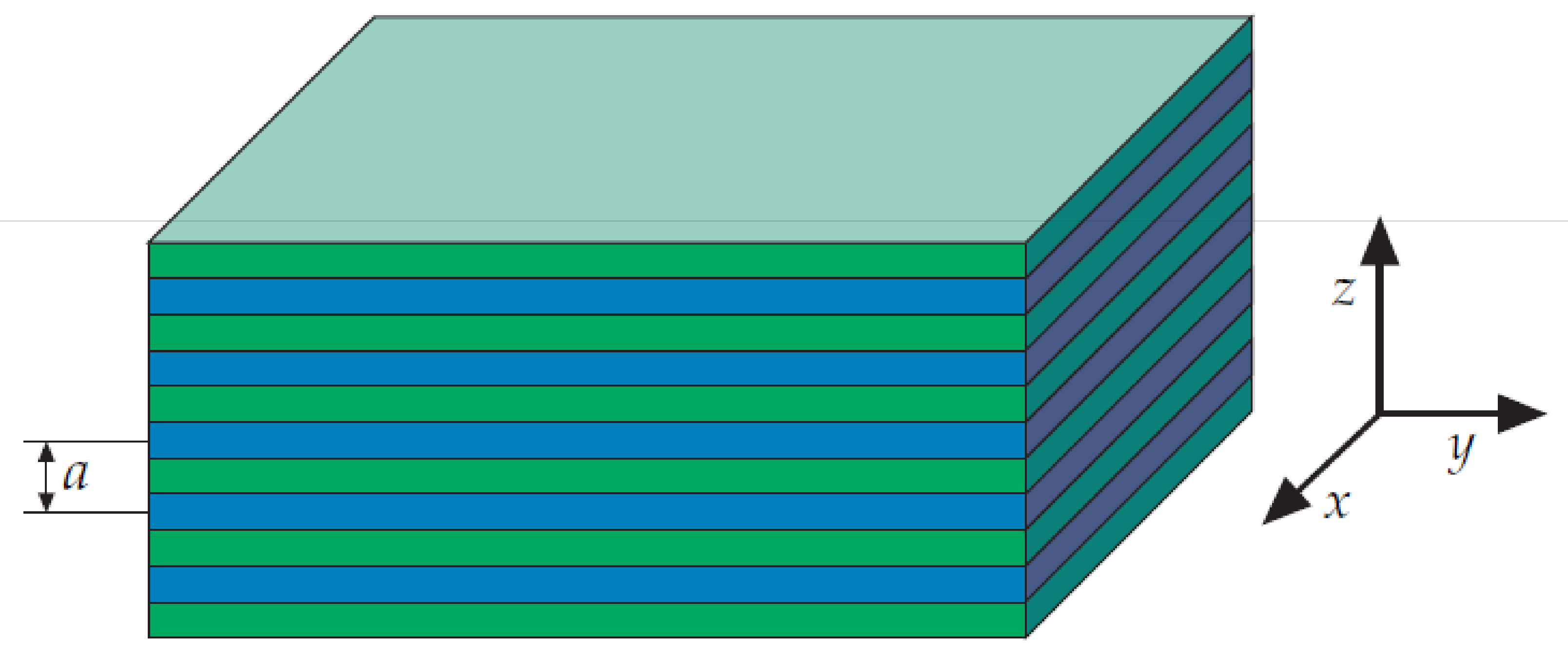

$$\mathbf{H}_{n,k_z,\mathbf{k}_\parallel}(\mathbf{r}) = e^{i\mathbf{k}_\parallel \cdot \boldsymbol{\rho}} e^{ik_z z} \mathbf{u}_{n,k_z,\mathbf{k}_\parallel}(z).$$

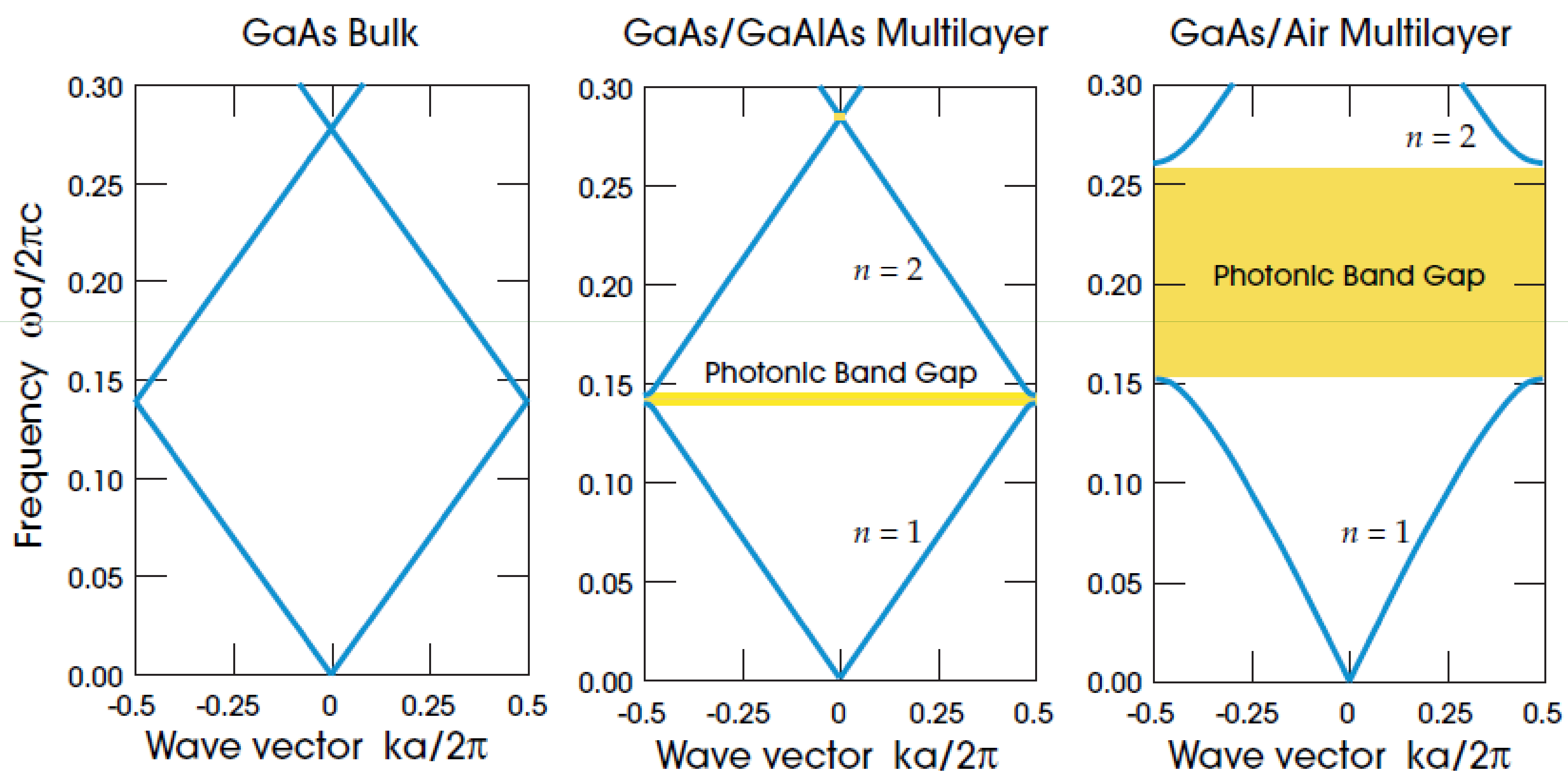

Figure 2: The photonic band structures for on-axis propagation, as computed for three different multilayer films. In all three cases, each layer has a width $0.5a$. *Left:* every layer has the same dielectric constant $\varepsilon = 13$. *Center:* layers alternate between ε of 13 and 12. *Right:* layers alternate between ε of 13 and 1.

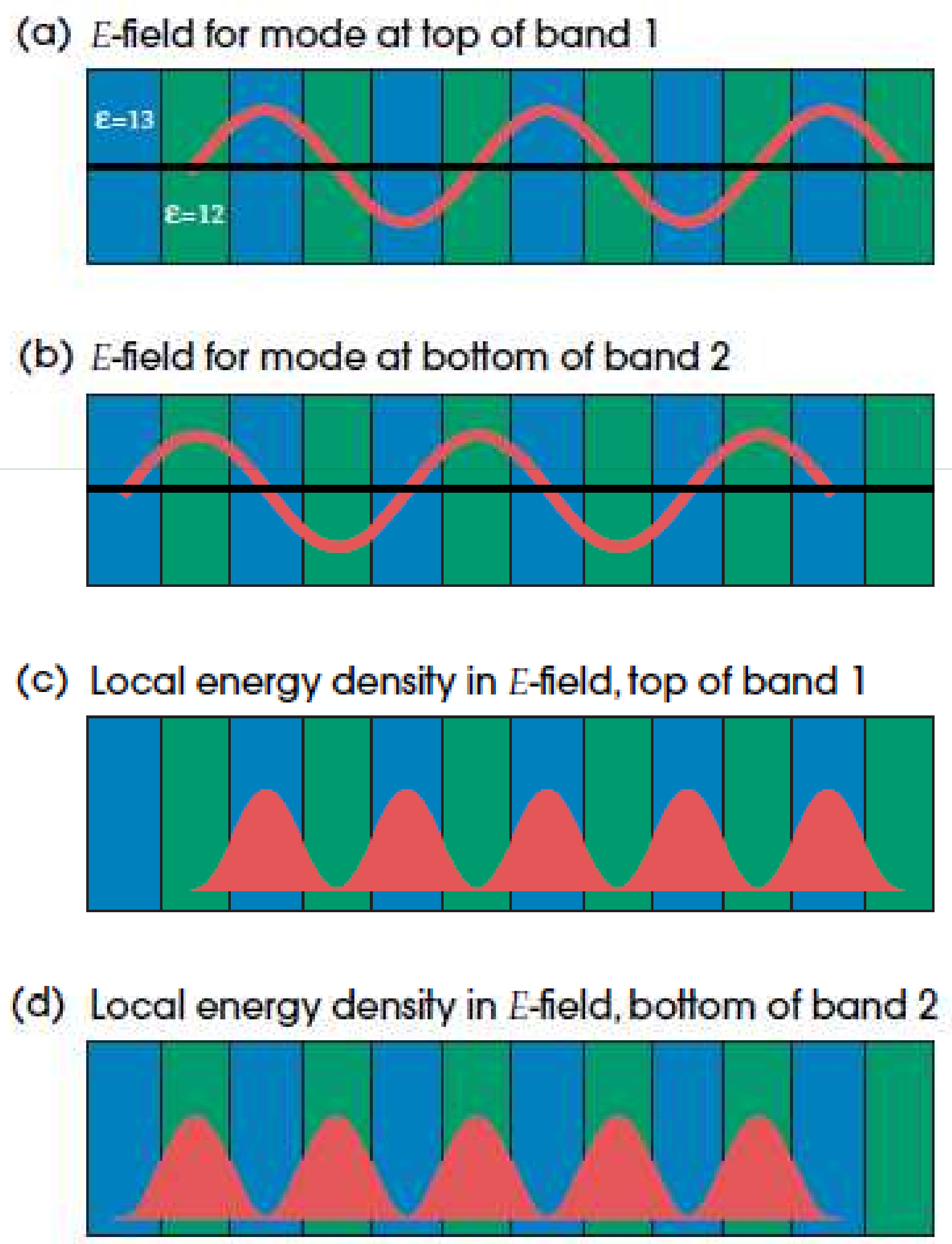
(a) E-field for mode at top of band 1
ε=13
ε=12
(b) E-field for mode at bottom of band 2
(c) Local energy density in E-field, top of band 1
(d) Local energy density in E-field, bottom of band 2

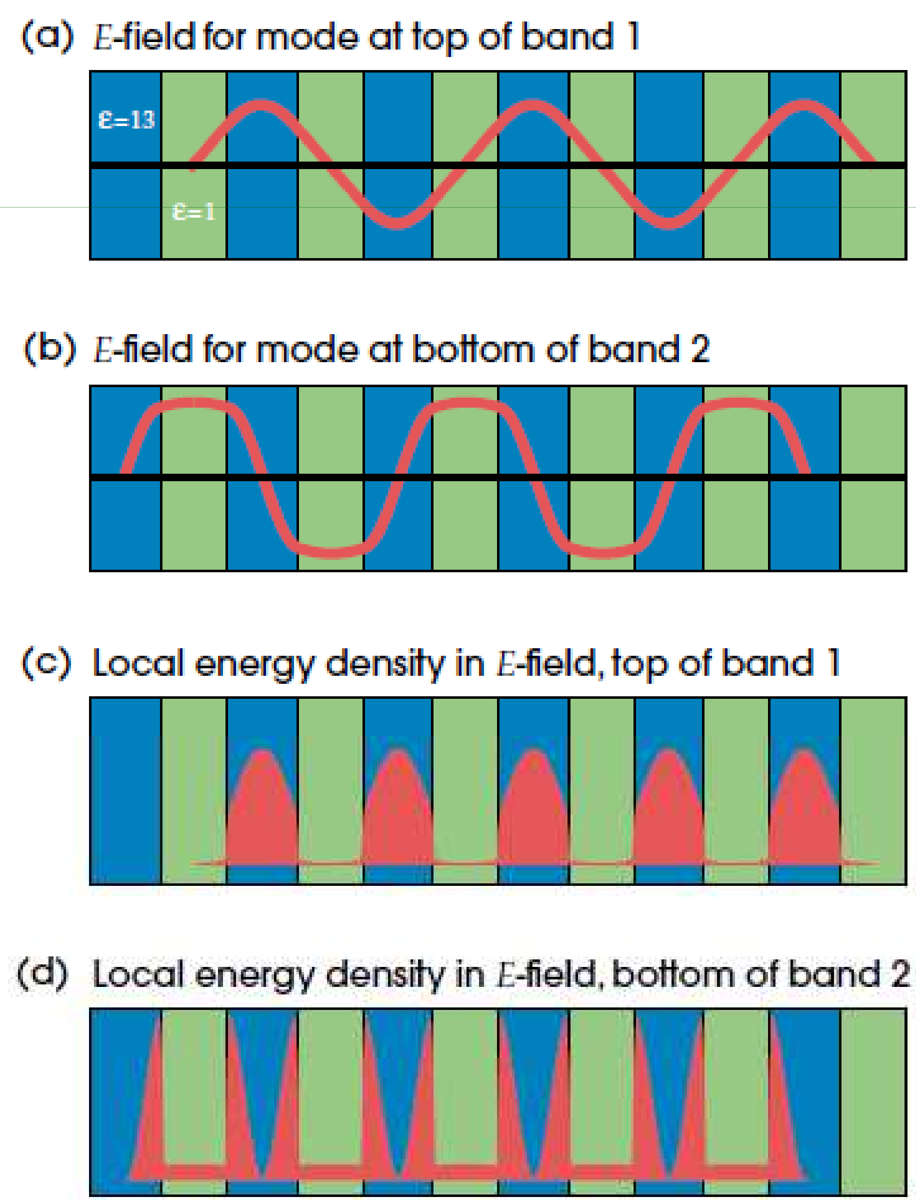
(a) E-field for mode at top of band 1
ε=13
ε=1
(b) E-field for mode at bottom of band 2
(c) Local energy density in E-field, top of band 1
(d) Local energy density in E-field, bottom of band 2

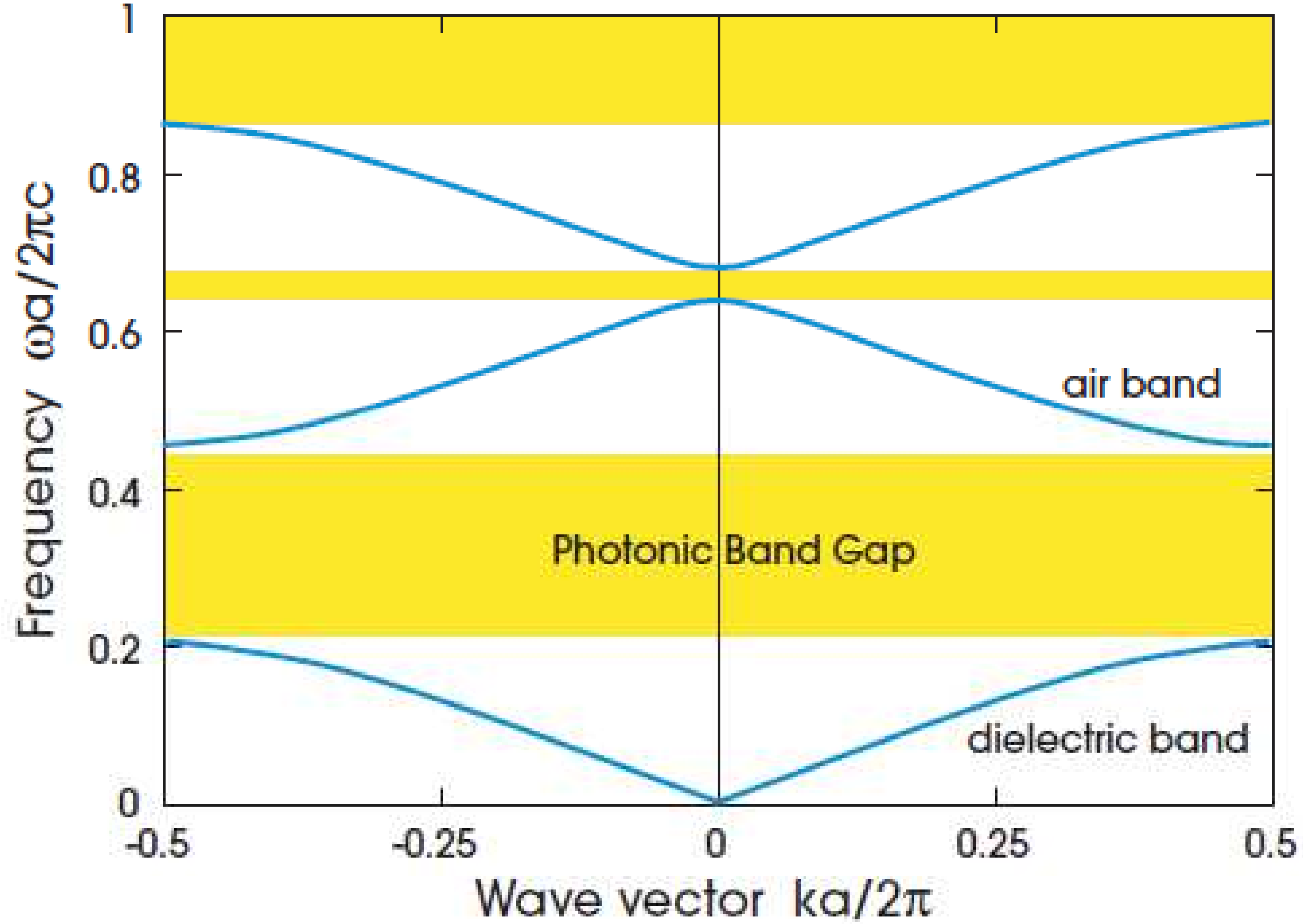

Figure 5: The photonic band structure of a multilayer film with lattice constant a and alternating layers of different widths. The width of the $\varepsilon = 13$ layer is $0.2a$, and the width of the $\varepsilon = 1$ layer is $0.8a$.

$$\frac{\Delta\omega}{\omega_m} \approx \frac{\Delta\varepsilon}{\varepsilon} \cdot \frac{\sin(\pi d/a)}{\pi}.$$

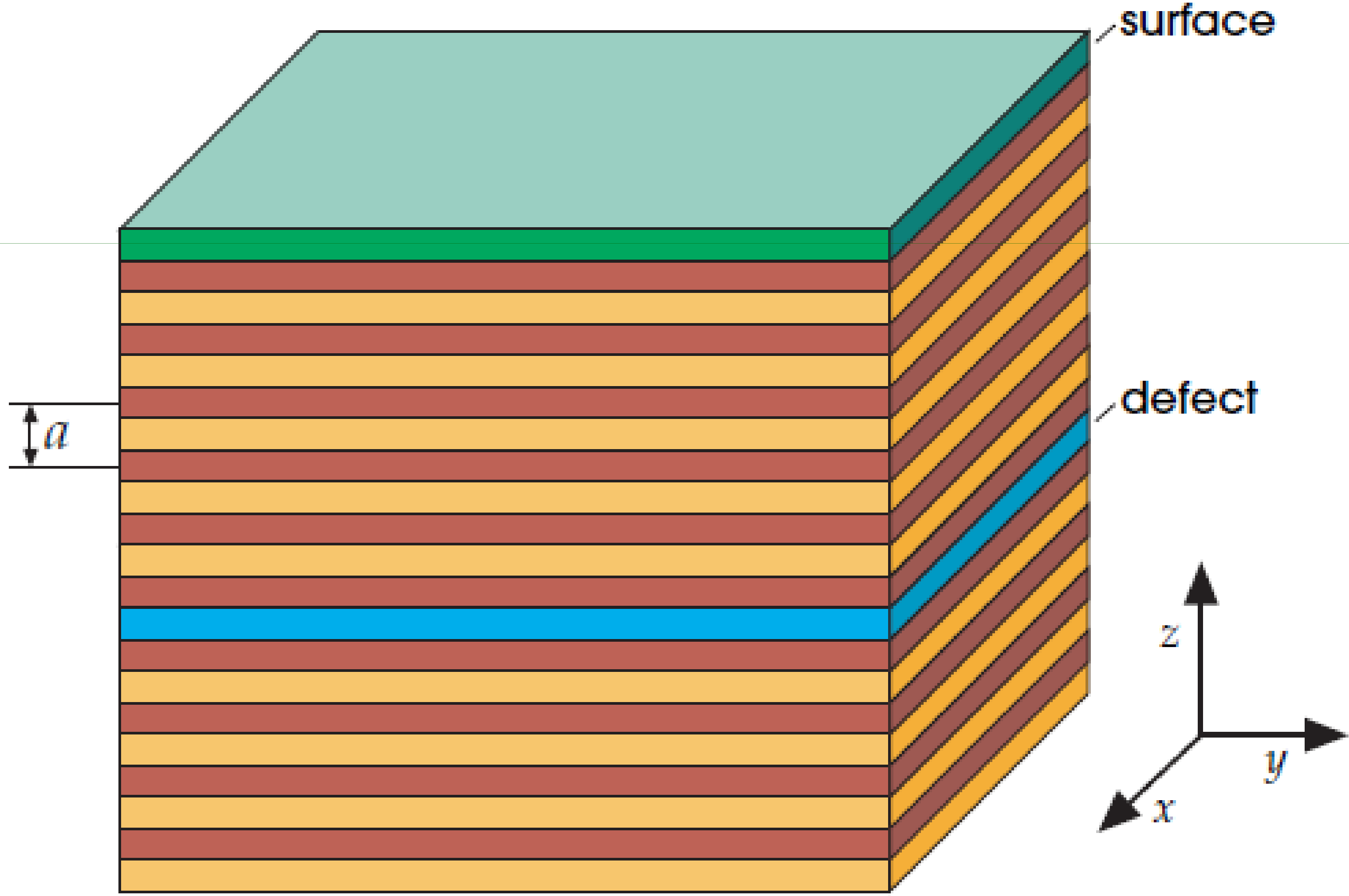
surface
defect
a
z
y
x

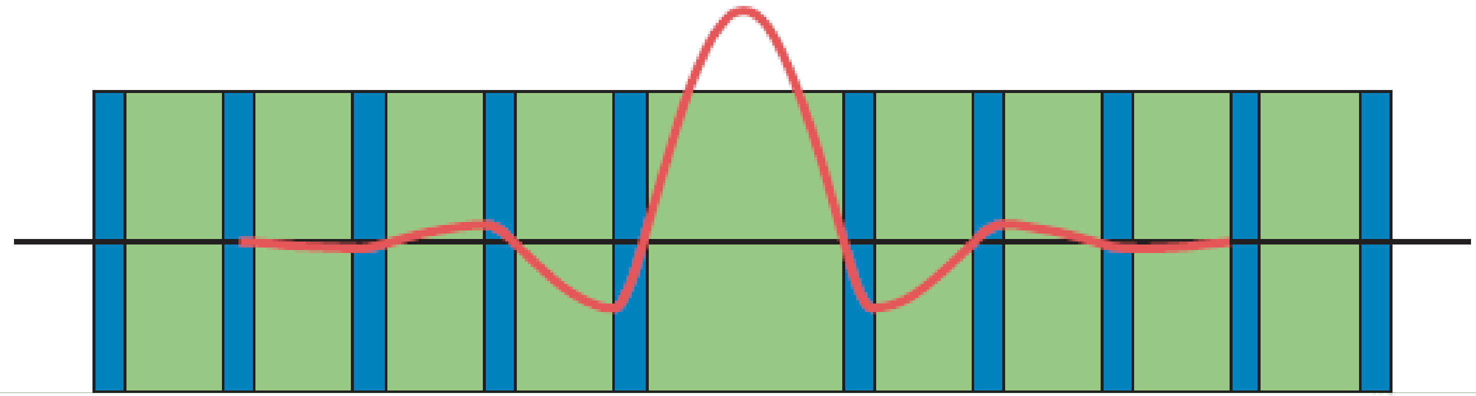

Figure 11: A defect in a multilayer film, formed by doubling the thickness of a single *low-ε* layer in the structure of figure 5. Note that this can be considered to be an interface between two perfect multilayer films. The red curve is the electric-field strength of the defect state associated with this structure (for on-axis propagation).

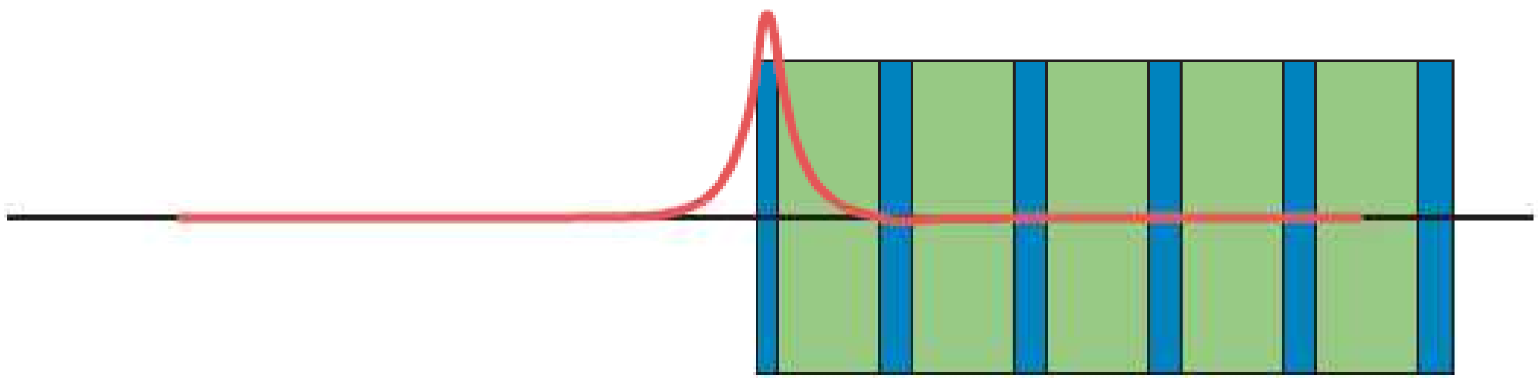

Figure 13: The electric field strength associated with a localized mode at the surface of a multilayer film. In particular, the mode at $k_y = 2\pi / a$ from figure 14 is shown. (This mode actually oscillates in sign with each period of the crystal, but with an amplitude too small to see clearly here.)

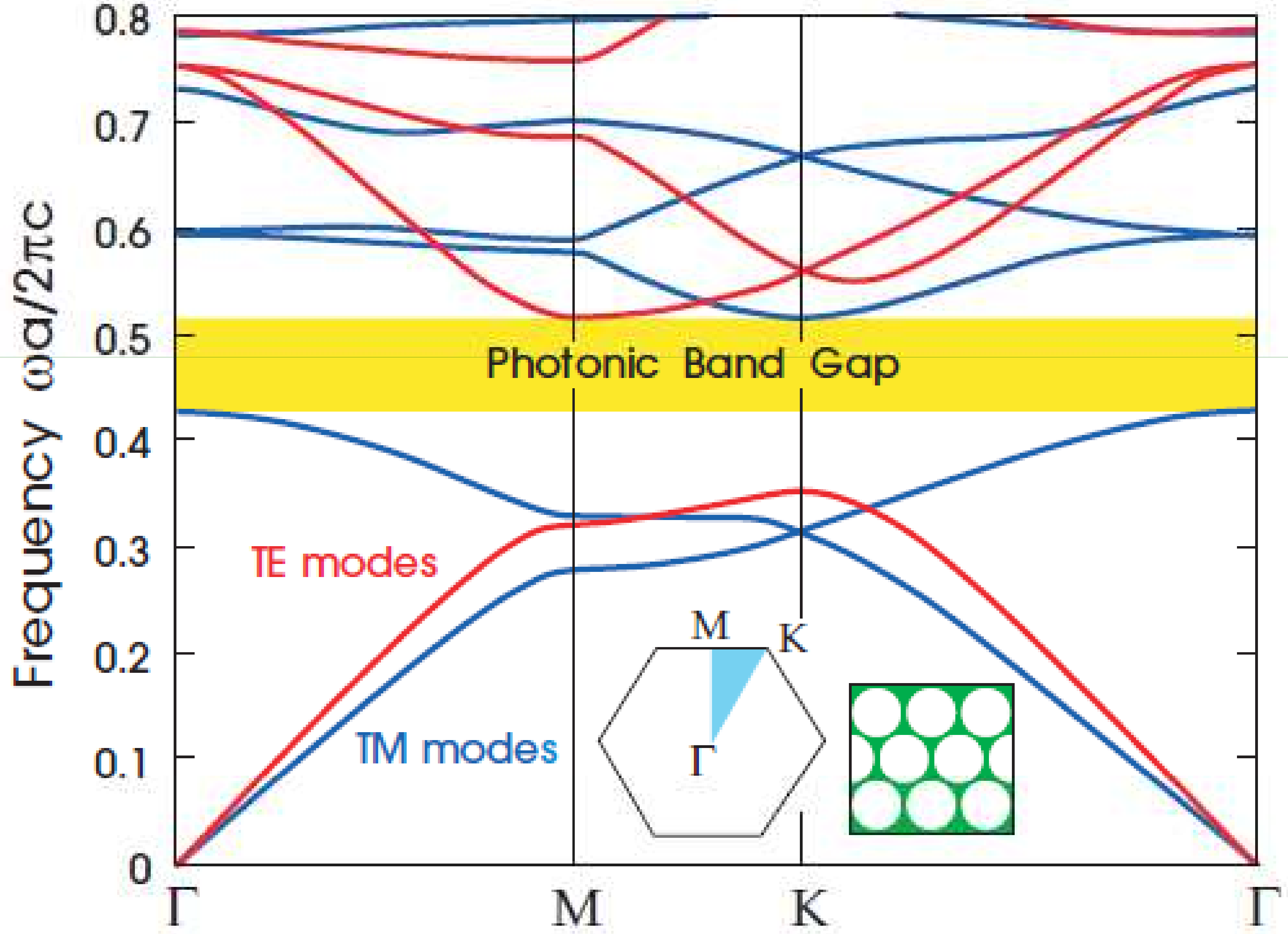

Figure 10: The photonic band structure for the modes of a triangular array of air columns drilled in a dielectric substrate ($\varepsilon = 13$). The blue lines represent TM bands and the red lines represent TE bands. The inset shows the high-symmetry points at the corners of the irreducible Brillouin zone (shaded light blue). Note the complete photonic band gap.

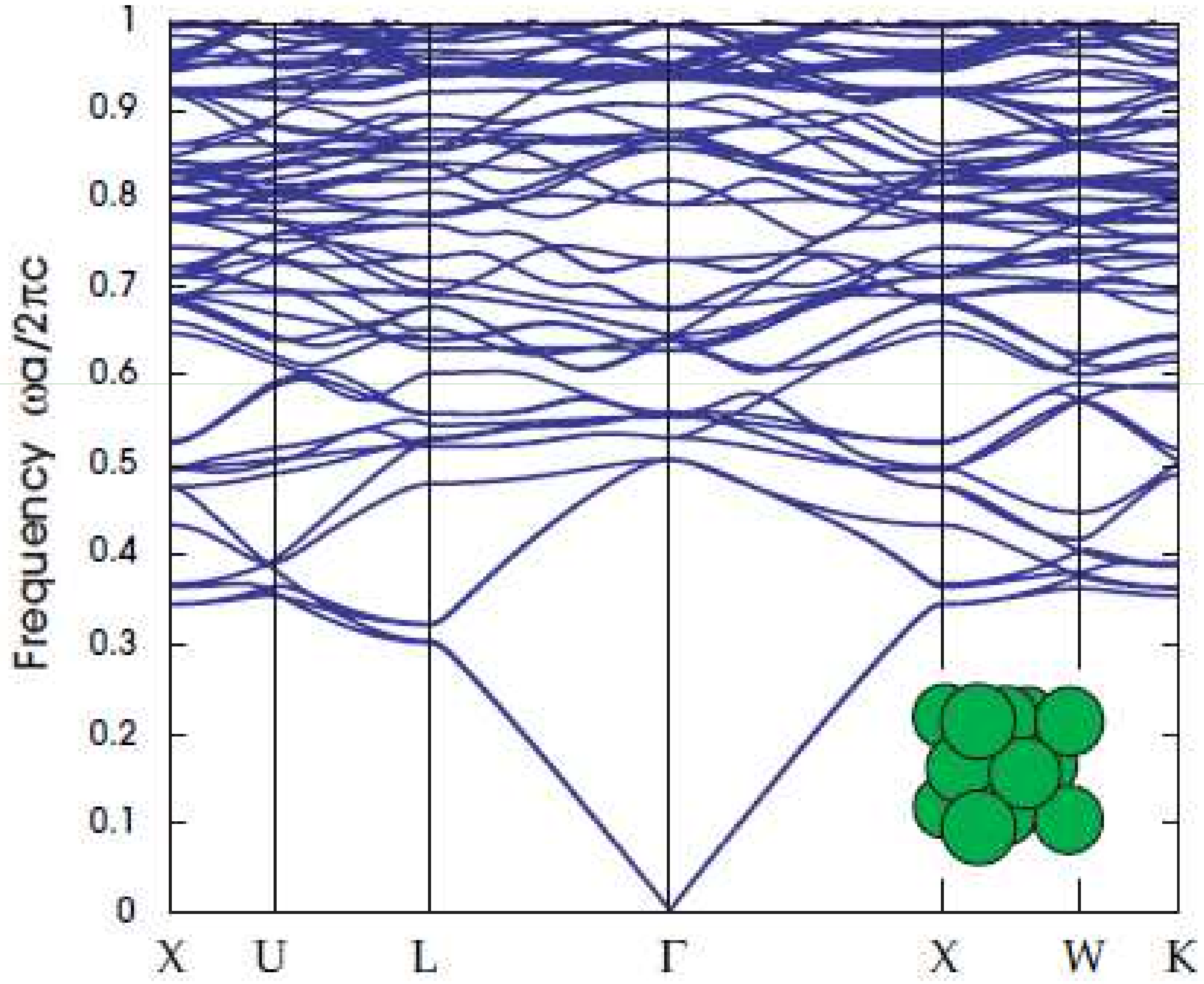

Figure 2: The photonic band structure for the lowest-frequency electromagnetic modes of a face-centered cubic (fcc) lattice of close-packed dielectric spheres ($\varepsilon = 13$) in air (inset). Note the *absence* of a complete photonic band gap. The wave vector varies across the irreducible Brillouin zone between the labelled high-symmetry points; see appendix B for a discussion of the Brillouin zone of an fcc lattice.

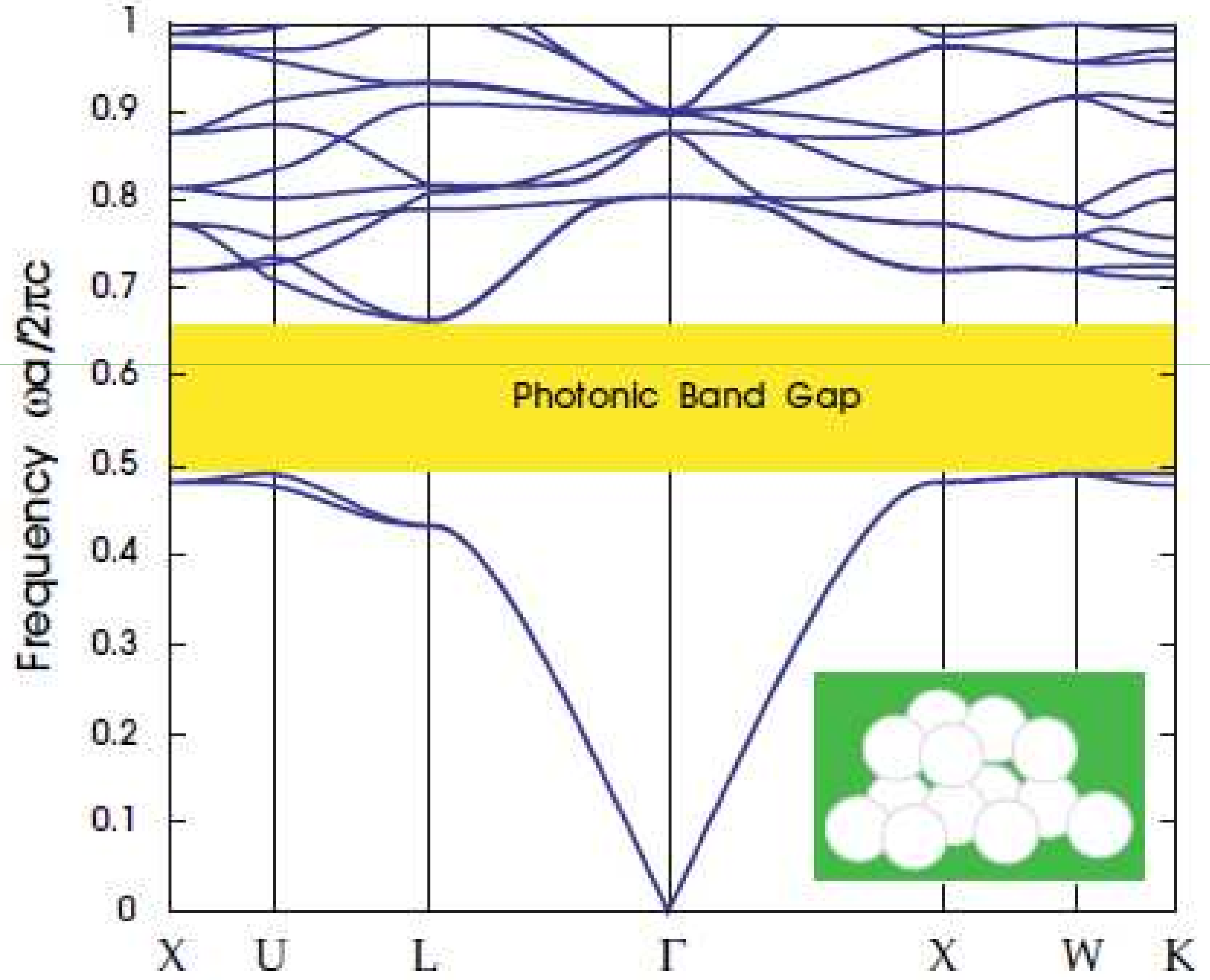

Figure 3: The photonic band structure for the lowest bands of a diamond lattice of air spheres in a high dielectric ($\varepsilon = 13$) material (inset). A complete photonic band gap is shown in yellow. The wave vector varies across the irreducible Brillouin zone between the labelled high-symmetry points; see appendix B for a discussion of the Brillouin zone of an fcc lattice.

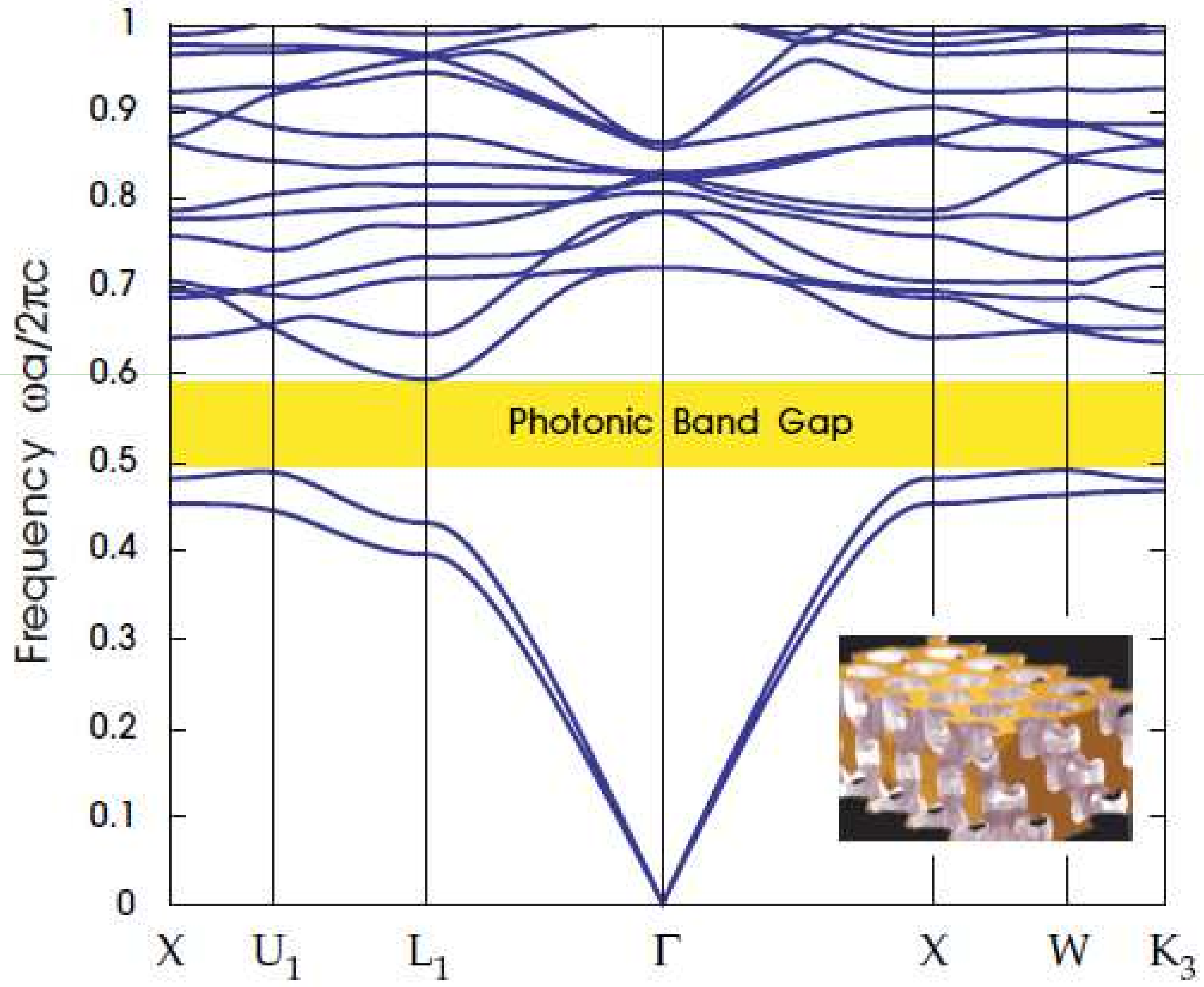

Figure 5: The photonic band structure for the lowest bands of Yablonovite (inset, from figure 4). Wave vectors are shown for a portion of the irreducible Brillouin zone that includes the edges of the complete gap (yellow). A detailed discussion of this band structure can be found in Yablonovitch et al. (1991*a*).

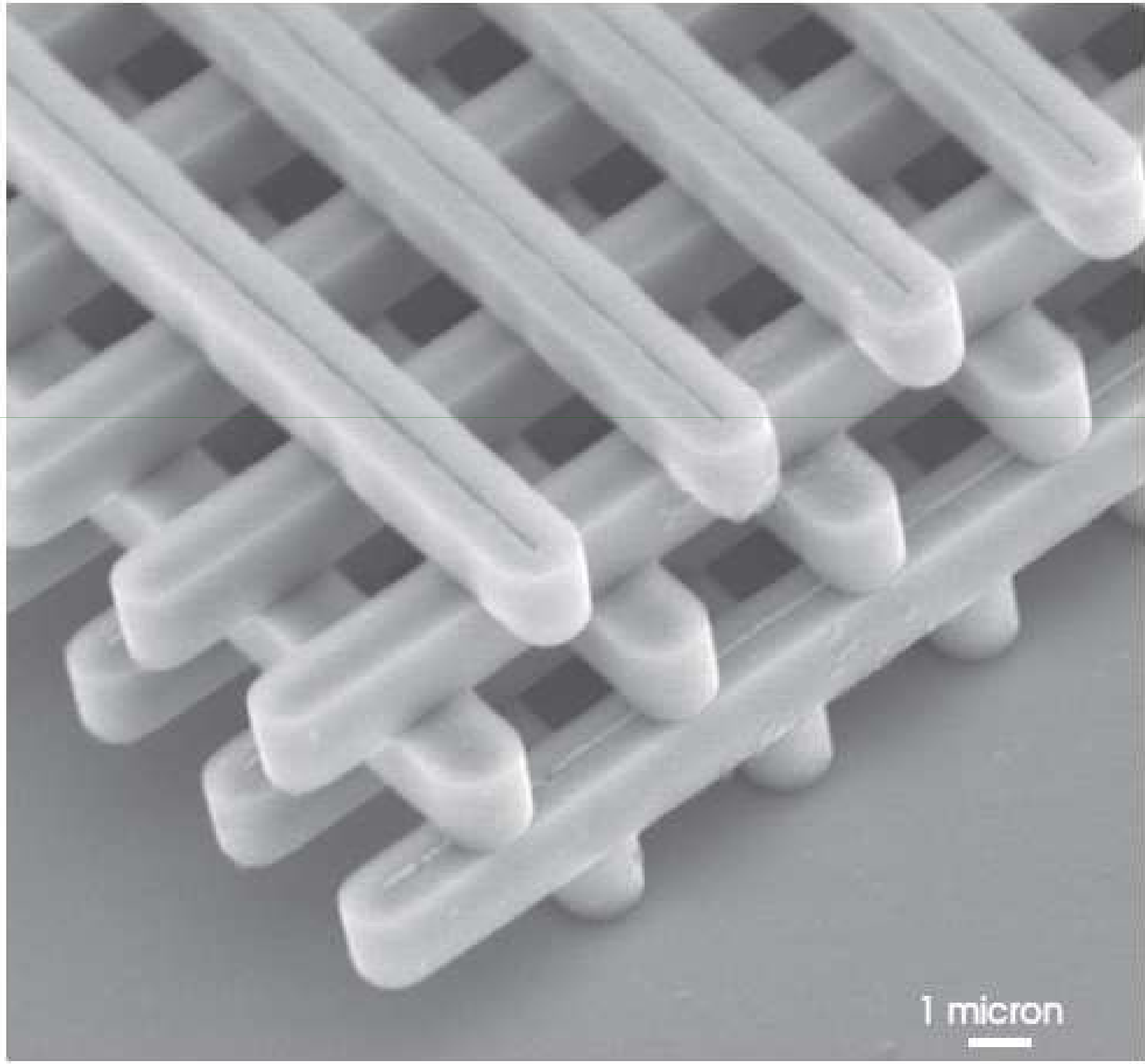

Figure 6: Electron-microscope image of a "woodpile" photonic crystal. The crystal is made of silicon and has a complete band gap centered at a wavelength of approximately 12 microns (Lin et al., 1998*b*). The dielectric "logs" form an fcc (or fct) lattice stacked in the [001] direction. (Image courtesy S.-Y. Lin.)

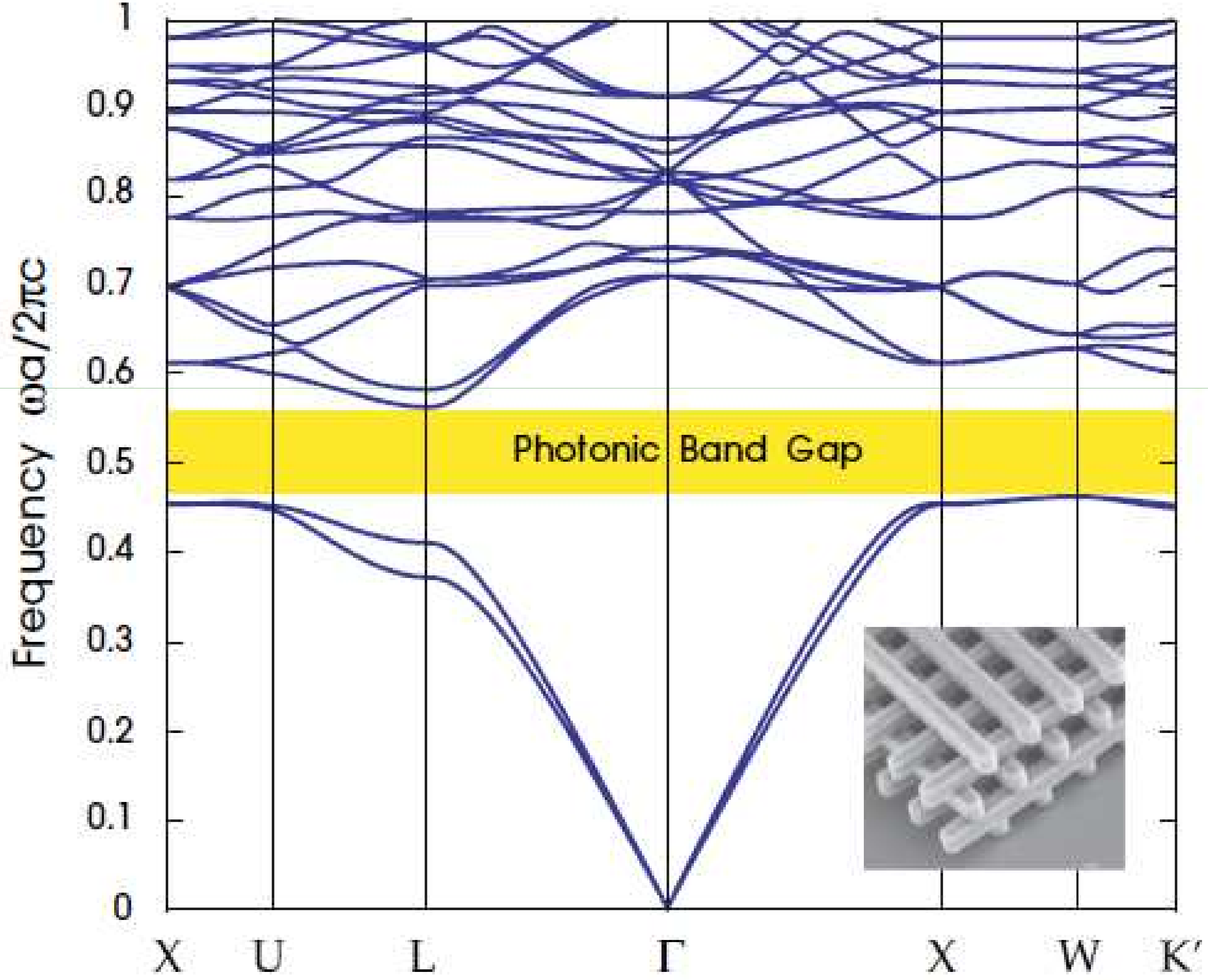

Figure 7: The photonic band structure for the lowest bands of the woodpile structure (inset, from figure 6) with $\varepsilon = 13$ logs in air. The irreducible Brillouin zone is larger than that of the fcc lattice described in appendix B, because of reduced symmetry—only a portion is shown, including the edges of the complete photonic band gap (yellow).

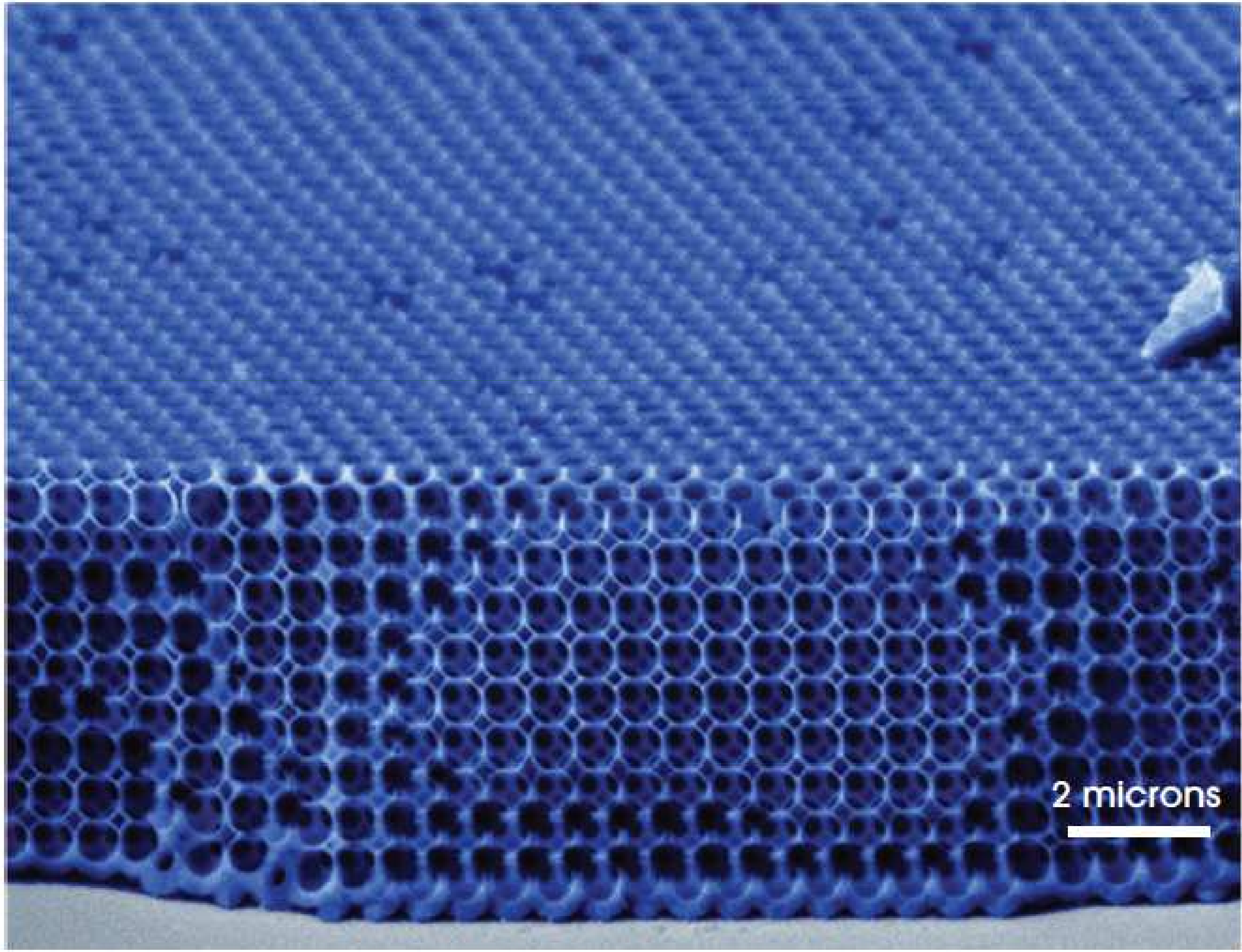

Figure 9: Electron-microscope image (artificial coloring) of inverse-opal structure demonstrated to have a complete band gap around a wavelength of 1.3 microns in Vlasov et al. (2001). Unlike figure 8, this is actually an fcc lattice of hollow dielectric (silicon) *shells*, which increases the size of the gap. (Image courtesy D. J. Norris.)

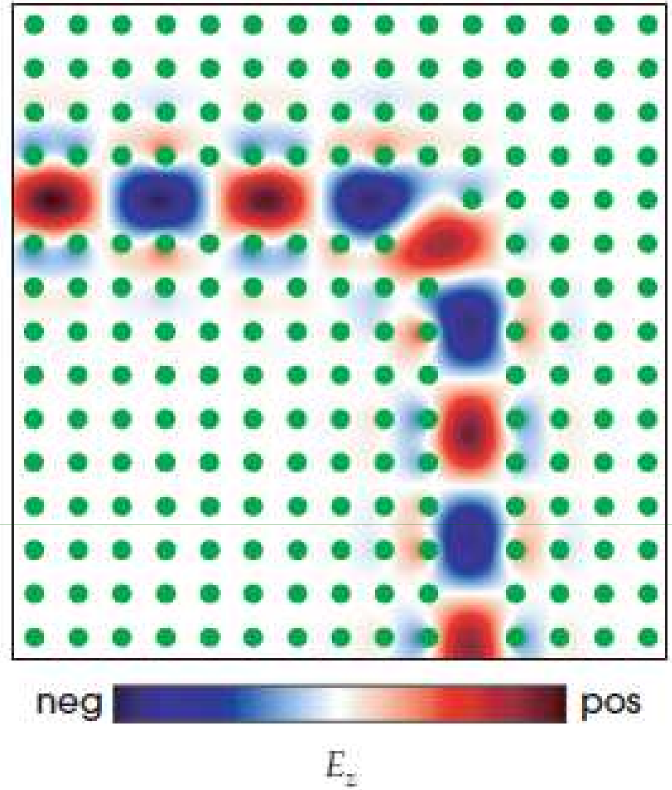
neg
pos
E_z

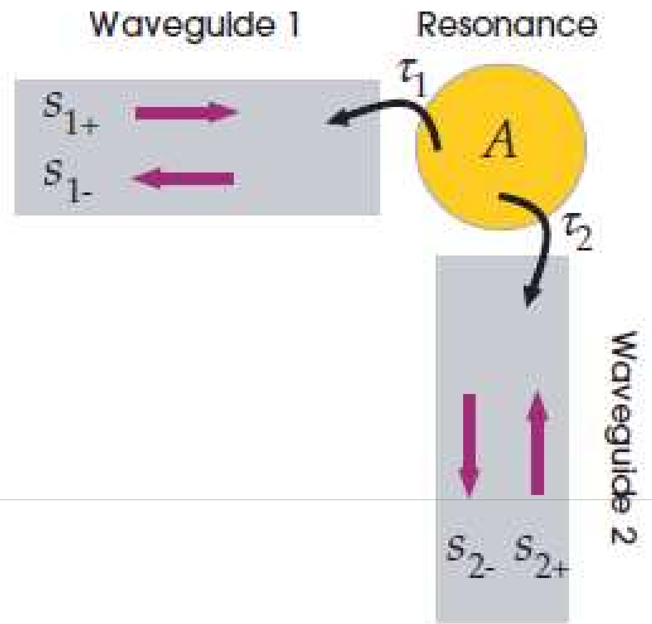
Waveguide 1
Resonance
s_{1+}
s_{1-}
τ_1
A
τ_2
Waveguide 2
s_{2-}
s_{2+}

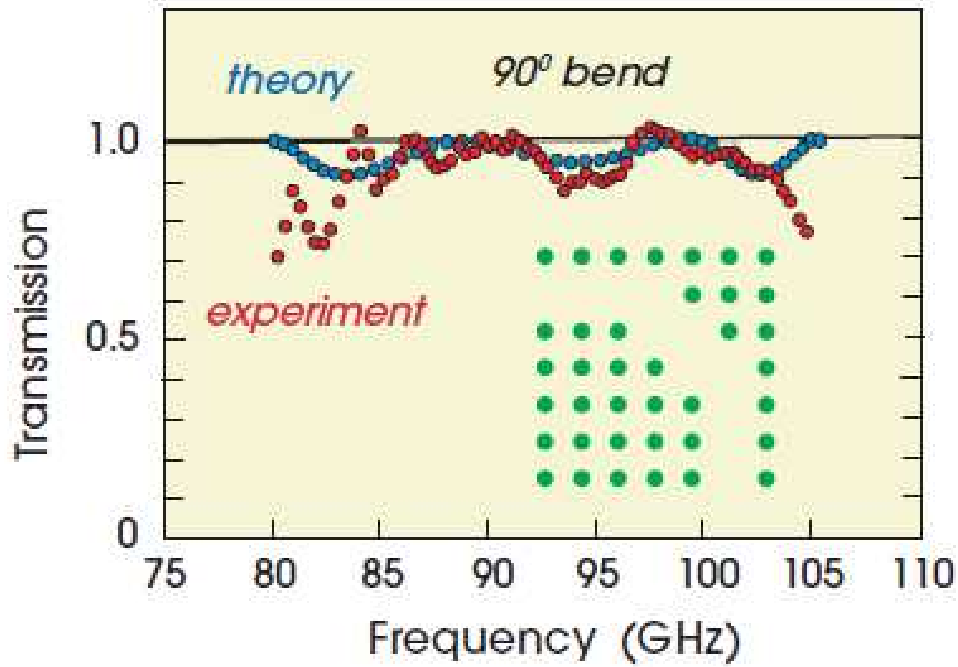
theory
90⁰ bend
experiment
Transmission
1.0
0.5
0
75
80
85
90
95
100
105
110
Frequency (GHz)

Photonic Crystals

Molding the Flow of Light

SECOND EDITION

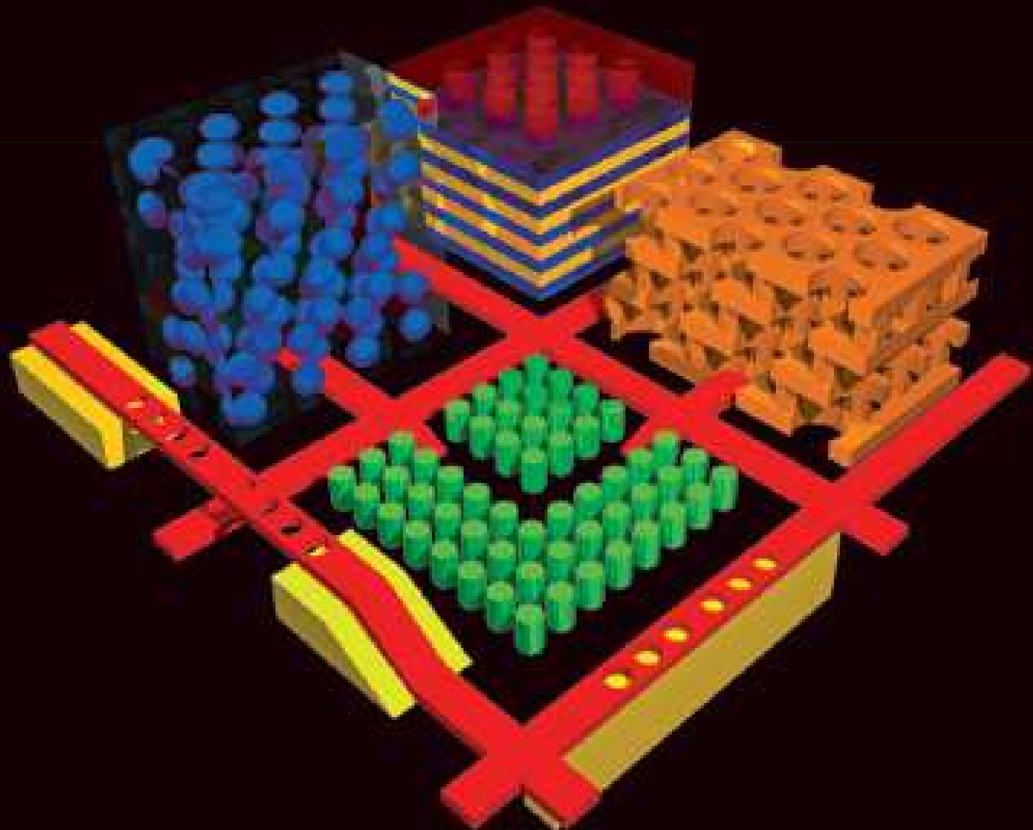

John D. Joannopoulos
Steven G. Johnson
Joshua N. Winn
Robert D. Meade